JACS
JOURNAL OF THE AMERICAN CHEMICAL SOCIETY
Article
pubs.acs.org/JACS

Graphane/Fluorographene Bilayer: Considerable C−H···F−C Hydrogen Bonding and Effective Band Structure Engineering

Yafei Li, Fengyu Li, and Zhongfang Chen*

Department of Chemistry, Institute for Functional Nanomaterials, University of Puerto Rico, Rio Piedras Campus, San Juan, Puerto Rico 00931

Supporting Information

ABSTRACT: Systematic density functional theory (DFT) computations revealed the existence of considerable C−H···F−C bonding between the experimentally realized graphane and fluorographene layers. The unique C−H···F−C bonds define the conformation of graphane/fluorographene (G/FG) bilayer and contribute to its stability. Interestingly, G/FG bilayer has an energy gap (0.5 eV) much lower than those of individual graphane and fluorographene. The binding strength of G/FG bilayer can be significantly enhanced by applying appropriate external electric field (E-field). Especially, changing the direction and strength of E-field can effectively modulate the energy gap of G/FG bilayer, and correspondingly causes a semiconductor−metal transition. These findings open new opportunities in fabricating new electronics and opto-electronics devices based on G/FG bilayer, and call for more efforts in using weak interactions for band structure engineering.

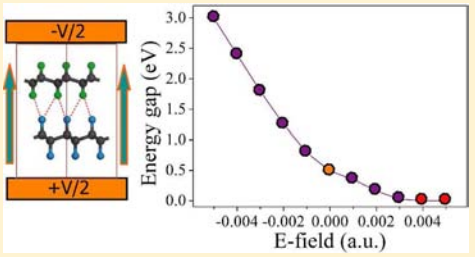

INTRODUCTION

Hydrogen bond, defined as the attractive interaction between a hydrogen atom (donor) and an electronegative atom (acceptor), such as nitrogen (N), oxygen (O), or fluorine (F), is operative in many chemical, physical, and biological structures and processes. This unique "site specific" interaction has been extensively explored especially since the 1980s.[1] According to Pauling's principle,[2] the strength of hydrogen bond (5−30 kJ/mol) increases as increasing the electronegativity of acceptor atom. Therefore, fluorine can form stronger bonding with hydrogen than other acceptor atoms due to its higher electronegativity.[3,4] Among these fluorine-containing hydrogen bonds, the C−H···F−C bond almost reaches the limit of hydrogen bonding.[5] Although the C−H···F−C interaction has been attracting many attentions from both experimental[6] and theoretical communities,[7] no consensus on this *"feeble"* bond had been achieved for a rather long time[8] until very recently: experimental studies[9,10] vigorously confirmed that C−H···F−C bonds, or even a single C−H···F−C bond, are strong enough to pair two molecules together and render them crystallographical difference in the solid state.

Since its experimental realization in 2004,[11] graphene, a single sheet of carbon atoms placed in honeycomb lattice, has been the focus of extensive studies.[12] Because of its excellent electronic[13] and mechanical properties,[14] graphene opens quite promising opportunities for the design of novel electronics devices, such as super-capacitors[15] and transparent conducting electrodes.[16] Especially since graphene has an ultrafast carrier mobility,[17] it is expected to replace silicon as the next-generation material used for microelectronics.[18] However, pristine graphene is zero-gap semimetal, and a considerable energy gap must be opened for the practical application of graphene in microelectronics devices.

Among various methods toward introducing a band gap to graphene,[19] such as chemical functionalization,[20] applying external electric field (E-field) to graphene bi- and tri-layers,[21,22] and uniaxial strain,[23] hydrogenation stands out since selective hydrogenation can well tune graphene's electronic and magnetic properties, as revealed by many theoretical[24,25] and experimental studies.[26,27] As a special case of the hydrogenated graphene, graphane (fully hydrogenated graphene) was first predicted theoretically by Sofo et al.,[24] and then was achieved experimentally by exposing graphene to hydrogen plasma,[28−30] or to atomic hydrogen generated by thermal cracking of molecular hydrogen,[31] or by dissociating hydrogen silsesquioxane on graphene.[32] A similar fully saturated graphene derivative is the fully fluorinated graphene (fluorographene), which was recently realized by exposing graphene to atomic F formed by decomposition of xenon difluoride (XeF_2).[33] Ever since its experimental realization, fluorographene has been extensively studied theoretically.[34] Graphane and fluorographene both have a wide energy gap (>3 eV),[24,35] which is a key advantage over graphene for their potential applications in electronics. However, for practical application, the energy gaps of graphane and fluorographene need to be decreased since most electronics and optoelectronics devices require semiconducting materials with energy gaps less than 3 eV.

Recently, with the development of theoretical methods, the weak interaction in layered materials, such as graphite[36−38] and

Received: April 26, 2012
Published: June 8, 2012

ACS Publications © 2012 American Chemical Society

dx.doi.org/10.1021/ja3040416 | J. Am. Chem. Soc. 2012, 134, 11269−11275

hexagonal BN,[39,40] V_2O_5,[41,42] can be well described. The role of van der Waals (vdW) interaction in anchoring the layers at a fixed distance has been established.[43] Quite recently, Echeverría et al.[44] also revealed that there exists subtle dihydrogen bond in alkanes. Inspired by this interesting finding, Fokin et al.[45] computationally demonstrated that there is strong interlayer bonding between multilayered graphanes, which is quite unexpected since it was believed that the C−H bonds of graphane are fully saturated and there is no chance for the formation of hydrogen bonding between graphane layers.[24]

Essentially, the C−H···F−C interaction should be stronger than the C−H···H−C interaction. Therefore, can we pair a graphane layer and a fluorographene layer together through the C−H···F−C bonding? If yes, can we tune the electronic properties of the parent monolayers and lead to a complex with a desirable energy gap? To our best knowledge, no attempts exist for using such weak interactions to tune the electronic properties of two-dimensional (2D) nanomaterials.

In this work, encouraged by the considerable C−H···F−C bonding interaction between small molecular model systems and the reduced HOMO−LUMO gap of the complex, we systematically investigated the interlayer distance, binding energy, stacking pattern, and electronic properties of graphane/fluorographene (henceforth G/FG) bilayers by means of vdW-corrected density functional theory (DFT) computations. We demonstrated that 2D graphane and fluorographene truly can be paired together, and that the C−H···F−C bonds play a rather important role in determining the interlayer distance of G/FG bilayer. Interestingly, G/FG bilayer has a much lower energy gap (0.5 eV) than graphane and fluorographene, suggesting the possibility of tuning the electronic properties of nanomaterials via weak C−H···F−C interactions. Such band structure engineering is partially attributed to the spontaneous interlayer polarization. Moreover, we also show that a semiconductor-metal transition can occur in G/FG bilayer by changing the strength and direction of external E-field.

COMPUTATIONAL DETAILS

For finite molecular models, full geometry optimizations, as well as electronic structure computations, were performed at the B97D[46] (D stands for dispersion) level of theory together with the 6-31G (d, p) basis set by using the Gaussian 09 package.[47] The accuracy of B97D for describing the weak interactions has been well established.[48−51] Single-point energies were evaluated at the Møller−Plesset second-order perturbation (MP2)[52] level of theory based on the B97D optimized structures with the same basis set.

For periodic systems, our DFT computations employed an all-electron method within a generalized gradient approximation (GGA) for the exchange-correlation term, as implemented in the DMol^3 code.[53] The double numerical plus polarization (DNP) basis set and PBE[54] functional with dispersion correction were adopted. For comparison, computations were also performed with the LDA-PWC[55] functional. The accuracy of DNP basis sets is comparable to that of People's 6-31G** basis set.[56] Since the weak interactions are not well described by standard PBE functional, we adopted a PBE+D (D stands for dispersion) approach with the Grimme vdW correction.[57] This approach is a hybrid semiempirical solution that introduces damped atom-pairwise dispersion correction of the form C_6R^{-6} in the DFT formalism. From the DFT ground state electron density and reference values of the free atoms, the C_6 coefficients and the vdW radii (R) can be directly determined. As a benchmark, the binding energies of graphite (64 meV/atom) and h-BN (84 meV/atom) computed at PBE+D are quite close to experimental (63 meV/atom for graphite)[58] and earlier theoretical[36,40] studies (56 and 86 meV/atom for graphite and h-BN, respectively).

In the above periodic boundary conditions (PBC) computations, self-consistent field (SCF) calculations were performed with a convergence criterion of 10^{-6} au on the total energy and electronic computations. To ensure high quality results, the real-space global orbital cutoff radius was chosen as high as 4.6 Å in all the computations. We set the x and y directions parallel and the z direction perpendicular to the graphane/fluorographene plane, and adopted a supercell length of 20 Å in the z direction. The Brillouin zone was sampled with a $6 \times 6 \times 1$ Γ centered k points setting in geometry optimizations, and a $25 \times 25 \times 1$ grid was used for electronic structure computations.

RESULTS AND DISCUSSION

Finite Molecular Model. To ascertain whether the C−H···F−C bonding interaction exists between graphane and fluorogaphene layers, we first examined the finite molecular models by using high level ab initio computations. $C_{13}H_{22}$ and $C_{13}F_{22}$, which represent the simplest graphane and fluorographene models, respectively, were chosen.

For the most stable configuration of $C_{13}H_{22}/C_{13}F_{22}$ system (Figure 1), the B97D approach yields a binding energy of 670 meV and an average H···F length of 2.58 Å, which is within the length range of a typical C−H···F−C bond.[8] At the same theoretical level (B97D), the binding energy of $C_{13}H_{22}/C_{13}F_{22}$ is larger than that of $C_{13}H_{22}$ dimer (536 meV, in good agreement with ref 45), which reflects the stronger interaction of C−H···F−C bonding than that of C−H···H−C bonding.

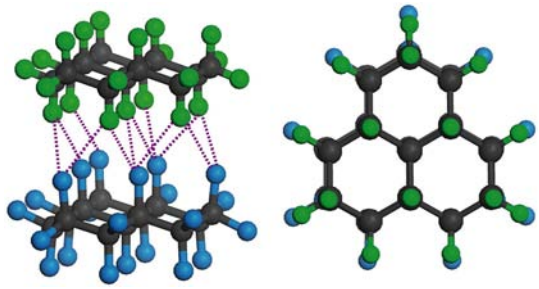

Figure 1. Side (left) and top (right) views of B97D optimized structure of $C_{13}H_{22}/C_{13}F_{22}$. The pink dashed lines denote the C−H···F−C bonding. The black, green, and indigo balls represent carbon, hydrogen, and fluorine atoms, respectively.

The reliability of the B97D approach to treat C−H···F−C interactions was validated by the very good agreement of the binding energies at B97D and MP2 levels for $C_{13}H_{22}/C_{13}F_{22}$ (670 vs 516 meV). In contrast, the pure B97 functional predicts a much lower binding energy (250 meV) with an overestimated average H···F length (2.80 Å).

To explore the effect of stacking to the electronic properties, the HOMO−LUMO gaps of $C_{13}H_{22}/C_{13}F_{22}$ as well as individual $C_{13}H_{22}$ and $C_{13}F_{22}$ molecules were then computed (Figure 2). $C_{13}H_{22}$ has a pronounced HOMO−LUMO gap of 7.85 eV; the HOMO is contributed by the C−C bonding state while the LUMO exhibits a strong delocalized feature. $C_{13}F_{22}$ has a HOMO−LUMO gap of 5.48 eV; the HOMO is a mix of C−C bonding state and F 2s orbital, and the LUMO is an antibonding state between C and F orbitals. When $C_{13}H_{22}$ and $C_{13}F_{22}$ are stacked together, $C_{13}H_{22}/C_{13}F_{22}$ has a remarkably reduced HOMO−LUMO gap of 3.39 eV. The HOMO of $C_{13}H_{22}/C_{13}F_{22}$ comes from $C_{13}H_{22}$, while the LUMO is mainly from $C_{13}F_{22}$. Such an orbital recombination consequently leads to a much reduced HOMO−LUMO gap for the complex.

dx.doi.org/10.1021/ja3040416 | J. Am. Chem. Soc. 2012, 134, 11269−11275

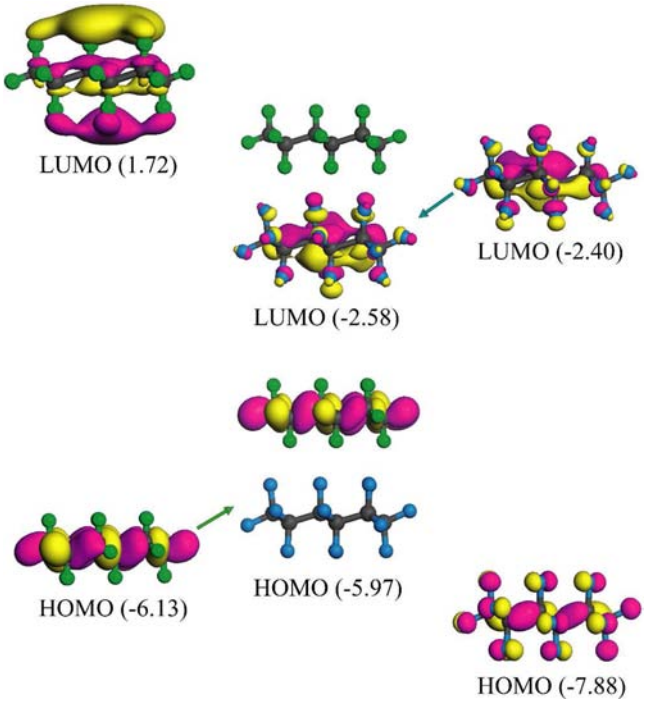

Figure 2. Charge densities of HOMO and LUMO for $C_{13}H_{22}/C_{13}F_{22}$ (middle), $C_{13}H_{22}$ (left), and $C_{13}F_{22}$ (right). The isovalue is 0.03 e/A^3.

Similar phenomenon has been observed in other hydrogen-bonded systems[59] and charge-transfer complexes.[60]

Note that the energy states of $C_{13}H_{22}/C_{13}F_{22}$ are not the simple superposition of energy states of the individual $C_{13}H_{22}$ and $C_{13}F_{22}$ molecules. The spontaneous intermolecular polarization also contributes to the reposition of the energy states, as indicated by the charge transfer of ~0.05 |e| from $C_{13}F_{22}$ to $C_{13}H_{22}$ obtained by the natural population analysis (NPA). This charge redistribution is a nature of vdW interaction system.[61]

Since we will use PBE-D for periodic systems in this work, we tested the performance of this approach for describing the C−H···F−C bonding for the above model systems. PBE-D gives the binding energy (410 meV) and H···F length (2.60 Å) comparable to those at B97D, thus, is capable of dealing with C−H···F−C bonding.

In addition to $C_{13}H_{22}/C_{13}F_{22}$, we also computed the binding energies and HOMO-LOMO gaps of several larger molecular models at the PBE-D theoretical level. It is found that the considerable C−H···F−C bonding interaction also exists in these larger models, and the binding energies increase linearly with increasing the model size. Similar to $C_{13}H_{22}/C_{13}F_{22}$, the orbital recombination holds true in these larger molecular models, and the HOMO−LUMO gaps decrease gradually with increasing of the model size (see Supporting Information).

The above comprehensive analyses demonstrate that there truly exists considerable C−H···F−C bonding interaction between molecular graphane and fluorographene, which significantly affects their electronic properties. These findings inspired us to explore the possibility to take advantage of these generally assumed weak C−H···F−C interactions to tune the electronic properties of more practical nanomaterials such as graphene. Moreover, we demonstrated that PBD+D can also well describe such weak interactions, and is a method of choice to treat larger periodic systems as below.

Infinite 2D G/FG Bilayer. *Geometric Structure.* Encouraged by above results, we constructed the infinite 2D G/FG bilayer by attaching a graphane monolayer and a fluorographene monolayer together. The energetically most favorable chair conformations[24,35] were adopted for both graphane and fluorographene. The length of unit cell of graphane (2.54 Å) is stretched by 2.4% to match that of fluorographene (2.60 Å).

There are four possible stacking patterns for G/FG bilayer (Figure 3). In patterns **I** and **II**, the carbon skeletons are in AA

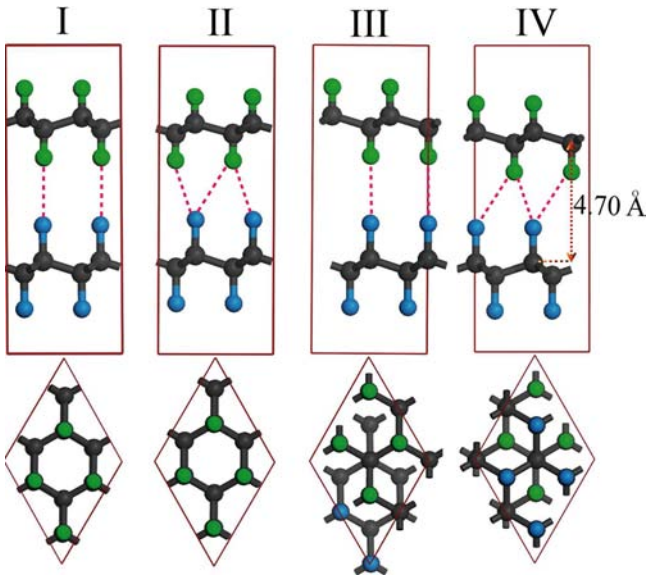

Figure 3. Side (upper) and top (bottom) views of ground state structure of G/FG bilayer in four stacking patterns. The double arrow in pattern **IV** denotes the interlayer distance.

stacking, while in patterns **III** and **IV**, the carbon skeletons have Bernal stacking feature (AB). Moreover, in patterns **I** and **III**, the H and F atoms between two carbon skeletons straightly point to each other, while in patterns **II** and **IV**, one H(F) atom points to the center site of three F(H) atoms.

Our computational results reveal that vdW correction has a significant effect on determining the global minimum of G/FG bilayer. Within the pure PBE functional pattern **III** is the global minimum; however, when the vdW correction is applied, the most stable configuration of G/FG bilayer adopts pattern **IV**, which is 20, 2, and 20 meV lower in energy than patterns **I**, **II**, and **III**, respectively (see Supporting Information). In the energetically most favorable pattern **IV**, PBE-D predicts a pronounced binding energy of 84 meV/unit cell, an interlayer distance (between two carbon skeleton) of 4.70 Å, and an average H···F length of 2.66 Å. The LDA-PWC approach also determines pattern **IV** as the global minimum, but yields a much lower binding energy (44 meV/unit cell) than PBE-D. At the same PBE-D theoretical level, the bind energy of the energetically most favorable G/FG bilayer (84 meV/unit cell) is larger than that of graphane bilayer (66 meV/unit cell), but lower than that of graphene bilayer (132 meV/unit cell) and *h*-BN bilayer (168 meV/unit cell). Note that only one C−H···F−H interaction is available in one unit cell in the G/FG bilayer, while there is a pair of p_π−p_π interaction in one unit cell of graphene bilayer, implying that σ−σ interaction is no less stable than π−π interaction. According to Hirshfeld charge population analysis, H atoms involved in C−H···F−C bonds are positively charged with ~0.01 |e| charge, while F atoms all carry a ~0.06 |

dx.doi.org/10.1021/ja3040416 | J. Am. Chem. Soc. 2012, 134, 11269−11275

el negative charge (see Supporting Information), thus, deriving the attractive electrostatic interaction. Totally, there is about 0.011−0.016 |e|/unit cell charge transfer from fluorographene to graphane in the four patterns of G/FG bilayer. Therefore, similar to $C_{13}H_{22}/C_{13}F_{22}$, there also exists a spontaneous interlayer polarization in G/FG bilayer in the direction from fluorographene to graphane.

Our above computations established that the C−H···F−C chemical bonding can hold the graphane and fluorographene layers together. However, why do patterns **II** and **IV** have the comparable binding energies, and are both more stable than patterns **I** and **III**? For all the four patterns, the C−H···F−C bonds in the G/FG bilayer are in the optimal range of 2.60−2.70 Å. To adopt this optimal bonding length, and thus enhance the C−H···F−C bonding, patterns **I** and **III** should have longer interlayer distances (5.10 Å) than those of patterns **II** and **IV** (4.70 Å), making the vdW correction for patterns **II** and **IV** more pronounced than those for patterns **I** and **III** since the vdW correction is inversely proportional to R^6. Therefore, it is the larger vdW correction that leads to the higher stability of patterns **II** and **IV**. We can conclude that the nature of C−H···F−C bonding directly determines the interlayer distance of G/FG bilayer, and results in the energy difference for the four patterns of G/FG bilayer.

Band Structure. How does this kind of stacking affect the electronic properties? To address this issue, we computed the band structure and density of states (DOS) of G/FG bilayer (Figure 4a). As a comparison, the electronic properties of graphane and fluorographene also were computed.

Graphane at its ground state has a wide direct energy gap of 4.60 eV. The elongation of lattice parameter by 2.4% (to match the lattice of fluorographene) further increases the energy gap of graphane to 5.00 eV (see Supporting Information). Fluorographene is also semiconducting with a direct energy gap of 3.43 eV.

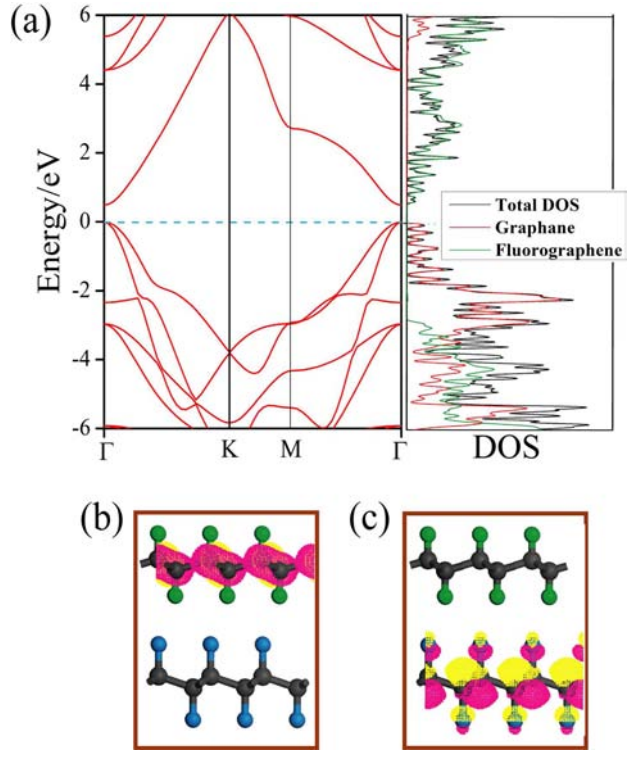

Figure 4. (a) Electronic band structure (left) and density of states (DOS, right) of G/FG bilayer. The Fermi level is assigned at 0 eV. (b and c) The partial charge densities of the (b) VBM and (c) CBM at the Γ point.. The isovalue is 0.03 e/A^3.

However, when graphane and fluorographene are paired together, the remarkable change occurs. The computed band structure shows that G/FG bilayer has a direct energy gap of only 0.50 eV, with the valence band maximum (VBM) and conduction band minimum (CBM) both located at the Γ point. The partial DOS analysis reveals that the states for the valence bands close to Fermi level are mainly contributed by graphane, while those for conduction bands come dominantly from fluorographene.

To get a deeper insight, we computed the partial charge densities of the VBM (Figure 4b) and the CBM (Figure 4c) at the Γ point for G/FG bilayer. The VBM is contributed by the carbon skeleton of graphane, while the CBM is from the carbon skeleton and fluorine atoms of fluorographene. Thus, the VBM and CBM of G/FG bilayer are localized on graphane and fluorographene, respectively. This alignment well resembles the $C_{13}H_{22}/C_{13}F_{22}$ model complex and leads to a low energy gap for G/FG bilayer. It also can be understood that pairing with fluorographene tunes graphane into a *p*-type semiconductor, or pairing with graphane tunes fluorographene into an *n*-type semiconductor.

Since the energy difference between different patterns is insignificant (20 meV/unit cell or less), we also computed the band structure of other three patterns of G/FG bilayer. Interestingly, all the patterns of G/FG bilayer have a similar band structure and a ∼0.50 eV energy gap, irrespective of the stacking pattern (see Supporting Information). Our studies suggest a rather flexible way toward reducing the wide energy gaps of graphane and fluorographene, which opens new opportunities in fabricating practical electronics and optoelectronics devices.

Effect of External E-Field to the Binding Strength and Band Structure. Applying external E-field has proven an efficient method toward tuning the electronic properties of graphene-related materials.[21,22,62] Recently, Zhou et al.[63] computationally revealed that the applied E-field can substantially enhance the interaction between H_2 molecules and polarizable materials (such as BN, silsesquioxane) by polarizing the H_2 molecules as well as the substrate. Inspired by these studies, we further examined the effect of E-field on the binding strength and electronic properties of G/FG bilayer in pattern **IV**. Two directions of E-field ($+z$, $-z$) perpendicular to the basal planes of graphane and fluorographene were considered. Here, we define the positive direction of the E-field as pointing from fluorographene to graphane (Figure 5a). The binding energy and charge transfer is plotted as a functional of the magnitude of the E-field in Figure 5b.

When E_{ext} is applied in the $+z$ direction, similar to the effect of spontaneous interlayer polarization as found above, the charge transfer from fluorographene to graphane increases monotonically with increase of the E-field strength. When E-field reaches 0.005 au, there is 0.056 |e|/unit cell charge transfer from fluorographene to graphane. Correspondingly, the binding energy is increased to 98 and 223 meV/unit cell at E-field = 0.001 and 0.005 au, respectively. When E-field is applied in the $-z$ direction, which is opposite to that of spontaneous interlayer polarization, the amount of charge transfer from fluorographene to graphene first decreases to 0.01 |e| at E-field = −0.001 au. At E-field = −0.002 au, fluorographene no longer

dx.doi.org/10.1021/ja3040416 | J. Am. Chem. Soc. 2012, 134, 11269−11275

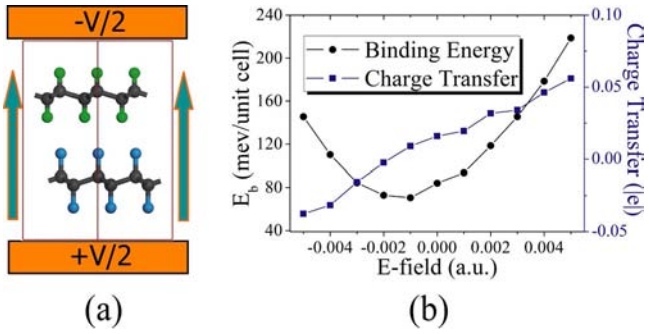

Figure 5. (a) Diagram of G/FG bilayer with the E-field. The positive direction of E-field is denoted by two arrows and the infinitely extended direction of G/FG bilayer is perpendicular to that of E-field. (b) Binding energy of G/FG bilayer and charge transfer from fluorographene to graphane as a function of E-field. The negative charge transfer denotes that charges are transferred from graphane to fluorographene.

donates charge to graphane; on the contrary, there is 0.002 |e| charge transfer from graphane to fluorographene. With further increase of E-field, more and more charge transfer from graphane to fluorographene occurs, and the value reaches 0.038 |e| at E-field = −0.005 au. Consequently, the binding energy first decreases to 72 meV/unit cell at E-field = −0.001 au, then increases with increasing E-field. When E-field reaches −0.005 au, a much enhanced binding strength (146 meV/unit cell) is achieved. These results demonstrate that the interaction between graphane and fluorographene can be significantly enhanced by applying appropriate external E-field.

The E-field has also a remarkable impact on the electronic properties of G/FG bilayer (Figure 6). Taking pattern **IV** as an

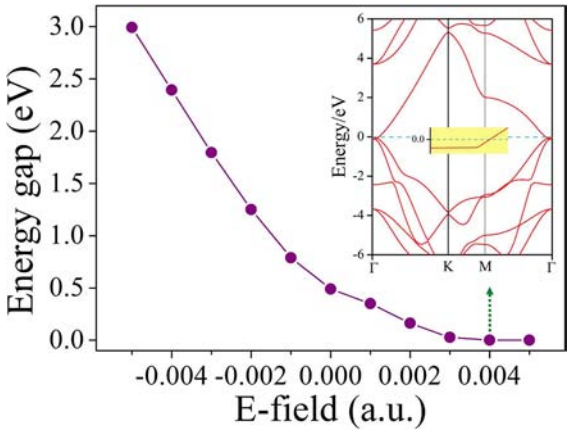

Figure 6. Energy gap of G/FG bilayer as a function of E-field. The inset figure is the band structure of G/FG bilayer at the E-field of 0.004 au. The zoom on the region around the Fermi level is also given.

example, under the positive E-field, the CBM shifts downward to the Fermi level gradually with increasing E-field, thus, further decreasing the energy gap. With an E-field of 0.004 au, the G/FG bilayer converts to be metallic, with an energy level crossing the Fermi level. In comparison, under the negative electric field, the CBM of G/FG bilayer shifts upward to the Fermi level as the strength of E-field increases, leading to an enlarged energy gap accordingly. When the E-field reaches −0.005 au, the energy gap of G/FG bilayer increases to 2.99 eV. In sharp contrast, the electronic properties of separated graphane or fluorographene monolayer are rather robust in response to E-field, since negligible modulation in the band structure is induced at the similar magnitude of E-field.

The similar modulation of energy gaps in response to electrical field as pattern **IV** holds true for other three patterns. The critical fields for the semiconducting to metallic transition are all estimated to be 0.004 au along the +z direction.

Thus, depending on the direction and strength of E-field, the energy gap of G/FG bilayer can be efficiently tuned, and the semiconductor−metal transition can be achieved. Especially the required electric field for effective band structure engineering is easily reachable experimentally.[21,22] Moreover, we are aware that GGA method usually underestimates the energy gap, and an accurate first-principles computation of energy gap requires the many-body perturbation theory (the GW method). Essentially, the upshift and downshift of CBM are driven by the charge redistribution among graphane and fluorographene, which would not be qualitatively affected by the GW self-energy correction. Therefore, the trend predicted here should not be changed though the GW correction would increase the threshold field for semiconducting-metallic transition.

CONCLUSION

In summary, our comprehensive theoretical computations first revealed considerable interactions between $C_{13}H_{22}$ and $C_{13}F_{22}$ molecules via C−H···F−C bonding, and then demonstrated the existence of such C−H···F−C interactions between 2D graphane and fluorographene (G/FG) bilayer. The nature of C−H···F−C bonds determines the interlayer distance and thus the stability of G/FG bilayer. Distinguished from individual graphane and fluorographene, both with a wide band gap, G/FG bilayer has a rather small energy gap (0.5 eV), suggesting a rather flexible way toward tuning the electronic properties of graphene derivatives. Under an appropriate external E-field, the binding strength of G/FG bilayer can be remarkably enhanced. Especially, the electronic properties of G/FG can be efficiently tuned from semiconductor to metal under an experimentally reachable E-field.

Our computations not only put forward the novel C−H···F−C chemical bonding into 2D periodic nanomaterial, but also identified a new effective approach to modulate the band structures. We strongly believe that the experimental peers can realize G/FG bilayer with small energy gaps very soon, tune their band structures with ease by using external fields, and employ them in novel integrated functional nanodevices. We hope that our studies will inspire more experimental and theoretical studies on using weak interactions to tune electronic properties of graphene-related materials.

ASSOCIATED CONTENT

Supporting Information

Complete citation of ref 47, the binding energies and HOMO−LUMO gaps of larger molecular models at PBE+D/DNP, the binding curves of G/FG bilayer in the stacking patterns **I**, **II**, and **III** as a function of interlayer distance, the atomic charge population of G/FG bilayer in four stacking patterns, the band structures of graphane and fluorographene, the band structures of G/FG bilayer in the stacking patterns **I**, **II**, and **III**, the energy gap of G/FG bilayer in the stacking pattern **I**, **II**, and **III** as a function of E-field. This material is available free of charge via the Internet at http://pubs.acs.org.

dx.doi.org/10.1021/ja3040416 | J. Am. Chem. Soc. 2012, 134, 11269−11275

AUTHOR INFORMATION

Corresponding Author

zhongfangchen@gmail.com

Notes

The authors declare no competing financial interest.

ACKNOWLEDGMENTS

Support by Department of Defense (Grant W911NF-12-1-0083) and NSF (Grant EPS-1010094) is gratefully acknowledged. This paper is dedicated to Professor Waldemar Adam on the occasion of his 75th birthday.

REFERENCES

(1) (a) Taylor, R.; Kennard, O. *Chem. Res.* **1984**, *17*, 320−326. (b) Etter, M. C. *Acc. Chem. Res.* **1990**, *23*, 120−126. (c) Desiraju, G. R. *Acc. Chem. Res.* **1996**, *29*, 441−449. (d) Gordon, M. S.; Jensen, J. H. *Acc. Chem. Res.* **1996**, *29*, 536−543. (e) Custelcean, R.; Jackson, J. E. *Chem. Rev.* **2001**, *101*, 1963−1980. (f) Desiraju, G. R. *Acc. Chem. Res.* **2002**, *35*, 565−573. (g) Patel, D. J.; Majumdar, A. *Acc. Chem. Res.* **2002**, *35*, 1−11. (h) Steiner, T. *Angew. Chem., Int. Ed.* **2002**, *41*, 48−76. (i) Borovik, A. S. *Acc. Chem. Res.* **2005**, *38*, 54−61. (j) Grabowski, S. J. *Chem. Rev.* **2011**, *111*, 2597−2625. (k) Han, K. L.; Zhang, G. J. *Acc. Chem. Res.* **2012**, *45*, 404−413.

(2) Pauling, L. C. *The Nature of the Chemical Bond*; Cornell University: New York, 1960.

(3) Howard, J. A. K.; Hoy, V. J.; Hagan, D. O.; Smith, G. T. *Tetrahedron* **1996**, *52*, 12613−12622.

(4) Espinasa, E.; Alkorta, I.; Elguero, J.; Molius, E. *J. Chem. Phys.* **2002**, *117*, 5529−5542.

(5) Desiraju, G. R.; Steiner, T. *The Weak Hydrogen Bond in Structural Chemistry and Biology*; Oxford University Press: Oxford, U.K., 1999, pp 205−209.

(6) (a) Golovanov, D. G.; Lyssenko, K. A.; Antipin, M. Yu.; Vygodskii, Y. S.; Lozinskaya, E. I.; Shaplov, A. S. *CrystEngComm* **2005**, *7*, 53−56. (b) Alonso, J. L.; Antolínez, S.; Blanco, S.; Lesarri, A.; López, J. C.; Caminat, W. *J. Am. Chem. Soc.* **2004**, *126*, 3244−3249. (c) Cocinero, E. J.; Sanchez, R.; Blanco, S.; Lesarri, A.; López, J. C.; Alonso, J. L. *Chem. Phys. Lett.* **2005**, *402*, 4−10. (d) Mori, Y.; Matsumoto, A. *Cryst. Growth Des.* **2007**, *7*, 377−385. (e) D'Oria, E.; Novoa, J. J. *CrystEngComm* **2008**, *10*, 423−436. (f) Ojala, W. H.; Skrypek, T. M.; MacQueen, B. C.; Ojala, C. R. *Acta Crystallogr.* **2010**, *66*, 565−570. (g) Anzahaee, M. Y.; Watts, J. K.; Alla, N. R.; Nicholson, A. W.; Damha, M. J. *J. Am. Chem. Soc.* **2011**, *133*, 728−731.

(7) (a) Kryspin, I. H.; Haufe, G.; Grimme, S. *Chem.−Eur. J.* **2004**, *10*, 3411−3422. (b) Prakash, G. K.; Wang, F.; Rahm, M.; Shen, J.; Ni, C.; Haiges, R.; Olag, G. A. *Angew. Chem., Int. Ed.* **2011**, *50*, 11761−11764. (c) Jabłoński, M; Palusiak, M. *J. Phys. Chem. A* **2012**, *116*, 2322−2332. (d) Scerba, M. T.; Bloom, S.; Haselton, N.; Siegler, M.; Jaffe, J.; Lectka, T. *J. Org. Chem.* **2012**, *77*, 1605−1609.

(8) Reichenbächer, K.; Süss, H. I.; Hulliger, J. *Chem. Roc. Rev.* **2005**, *34*, 22−30.

(9) Althoff, G.; Ruiz, J.; Rodriguez, V.; Lopez, G.; Perez, J.; Janiak, C. *CrystEngComm* **2006**, *8*, 662−665.

(10) Thakur, T. S.; Kirchner, M. T.; Bläser, D.; Boese, R.; Desiraju, G. R. *CrystEngComm* **2010**, *12*, 2079−2085.

(11) (a) Novoselov, K. S.; Geim, A. K.; Morozov, S. V.; Jiang, D.; Zhang, Y.; Dubonos, S. V.; Gregorieva, I. V.; Firsov, A. *Science* **2004**, *306*, 666−669. (b) Novoselov, K. S.; Jiang, D.; Schedin, F.; Booth, T. J.; Khotkevich, V. V.; Morozov, S. V.; Geim, A. K. *Proc. Natl. Acad. Sci. U.S.A.* **2005**, *102*, 10451−10453.

(12) For some very recent reviews, see (a) Allen, M. J.; Tung, V. C.; Kaner, R. B. *Chem. Rev.* **2010**, *110*, 132−145. (b) Castro Neto, A. H.; Novoselov, K. *Rep. Prog. Phys.* **2011**, *74*, 082501. (c) Rao, C. N. R.; Subrahmanyam, K. S.; Matte, H. S. S. R.; Govindaraj, A. *Mod. Phys. Lett. B* **2011**, *25*, 427−451. (d) Guo, S.; Dong, S. *Chem. Soc. Rev.* **2011**, *40*, 2644−2672. (e) Terrones, M.; Botello-Mendez, A. R.; Campos-Delgado, J.; Lopez-Urias, F.; Vega-Cantu, Y. I.; Rodriguez-Macias, F. J.; Elias, A. L.; Munoz-Sandoval, E.; Cano-Marquez, A. G.; Charlier, J.-C.; Terrones, H. *Nano Today* **2010**, *5*, 351−372.

(13) Novoselov, K. S.; Geim, A. K.; Morozov, S. V.; Jiang, D.; Khotkevich, I. V.; Gregorieva, I. V.; Dubonos, S. V.; Firsov, A. A. *Nature* **2005**, *438*, 197−200.

(14) Lee, C. G.; Wei, X. D.; Kysar, J. W.; Hone, J. *Science* **2008**, *321*, 385−388.

(15) Stoller, M. D.; Park, S.; Zhu, Y.; An, J.; Ruoff, R. S. *Nano Lett.* **2008**, *8*, 3498−3502.

(16) Sordan, R.; Traversi, F.; Russo, V. *Appl. Phys. Lett.* **2009**, *94*, 073305.

(17) Morozov, S. V.; Novoselov, K. S.; Katsnelson, M. I.; Schedin, F.; Elias, D.; Jaszczak, J. A.; Geim, A. K. *Phys. Rev. Lett.* **2008**, *100*, 016602.

(18) Lemme, M. C.; Echtermeyer, T. J.; Baus, M.; Kurz, H. *IEEE Electron Device Lett.* **2007**, *28*, 282−284.

(19) Castro Neto, A. H.; Guinea, F.; Peres, N. M. R.; Novoselov, K. S.; Geim, A. K. *Rev. Mod. Phys.* **2009**, *81*, 109−162.

(20) (a) Boukhvalov, D. W.; Katsnelson, M. I. *J. Phys.: Condens. Matter.* **2009**, *21*, 344205. (b) Klintenberg, M.; Lebègue, S.; Katsnelson, M. I.; Eriksson, O. *Phys. Rev. B* **2010**, *81*, 085433. (c) Tang, S. B.; Cao, Z. X. *J. Phys. Chem. C* **2012**, *116*, 8778−8791.

(21) Zhang, Y. B.; Tang, T. T.; Girit, C.; Zhao, H.; Martin, M. C.; Zettl, A.; Crommie, M. F.; Shen, Y. R.; Wang, F. *Nature* **2009**, *459*, 820−823.

(22) Lui, C. H.; Li, Z. Q.; Mak, K. F.; Capppeluti, E.; Heinz, T. F. *Nat. Phys.* **2011**, *7*, 944−947.

(23) Gyunea, F.; Katsnelson, M. I.; Geim, A. K. *Nat. Phys.* **2010**, *6*, 30−33.

(24) Sofo, J. O.; Chaudhari, A. S.; Barber, G. D. *Phys. Rev. B* **2007**, *75*, 153401.

(25) (a) Boukhvalov, D. W.; Katsnelson, M. I.; Lichtenstein, A. I. *Phys. Rev. B* **2008**, *77*, 035427. (b) Singh, A. K.; Yakobson, B. I. *Nano Lett.* **2009**, *9*, 1540−1543. (c) Wu, M.; Wu, X.; Gao, Y.; Zeng, X. C. *Appl. Phys. Lett.* **2009**, *94*, 223111. (d) Xiang, H. J.; Kan, E. J.; Wei, S. H.; Whangbo, M. H.; Yang, J. L. *Nano Lett.* **2009**, *9*, 4025−4030. (e) Samarakoon, D. K.; Wang, X. Q. *ACS Nano* **2009**, *3*, 4017−4022. (f) Lu, N.; Li, Z. Y.; Yang, J. L. *J. Phys. Chem. C* **2009**, *113*, 16741−16746. (g) Wu, M.; Wu, X.; Gao, Y.; Zeng, X. C. *J. Phys. Chem. C* **2010**, *114*, 139−142. (h) Singh, A. K.; Penev, E. S.; Yakobson, B. I. *ACS Nano* **2010**, *4*, 3510−3514. (i) Tang, S. B.; Cao, Z. X. *Chem. Phys. Lett.* **2010**, *488*, 67−72. (j) Şahin, H.; Ataca, C.; Ciraci, S. *Appl. Phys. Lett.* **2010**, *95*, 222510. (k) Şahin, H.; Ataca, C.; Ciraci, S. *Phys. Rev. B* **2010**, *81*, 205417. (l) Li, Y.; Chen, Z. *J. Phys. Chem. C* **2012**, *116*, 4526−4534. (m) Ma, Y. D.; Dai, Y.; Guo, M.; Niu, C. W.; Zhang, Z. L.; Huang, B. B. *Phys. Chem. Chem. Phys.* **2012**, *14*, 3651−3658.

(26) Haberer, D.; Guusca, C. E.; Wang, Y.; Sachdev, H.; Fedorov, A. V.; Farjam, M.; Jafari, S. A.; Vyalikh, D. V.; Usachov, D.; Liu, X. J. *Adv. Mater.* **2011**, *23*, 4497−4503.

(27) Balog, R.; Jørgensen, B.; Nilsson, L.; Andersen, M.; Rienks, E.; Bianchi, M.; Fanetti, M.; Lægsgaard, E.; Baraldi, A.; Lizzit, S.; Sljivancanin, Z.; Besenbacher, F.; Hammer, B.; Pedersen, T. G.; Hofmann, P.; Hornekær, L. *Nat. Mater.* **2010**, *9*, 315−319.

(28) Elias, D. C.; Nair, R. R.; Mohiuddin, T. M. G.; Morozov, S. V.; Blake, P.; Halsall, M. P.; Ferrari, A. C.; Boukhvalov, D. W.; Katsnelson, M. I.; Geim, A. K.; Novoselov, K. S. *Science* **2009**, *323*, 610−613.

(29) Xie, L.; Jiao, L.; Dai, H. *J. Am. Chem. Soc.* **2010**, *132*, 14751.

(30) Luo, Z.; Yu, T.; Kim, K. J.; Ni, Z.; You, Y.; Lim, S.; Shen, Z.; Lin, J. *ACS Nano* **2009**, *7*, 1781.

(31) Haberer, D.; Vyalikh, D. V.; Taioli, S; Dora, B.; Farjam, M.; Fink, J.; Marchenko, D.; Pichler, T.; Ziegler, K; Simonucci, S.; Dresselhaus, M. S.; Knupfer, M.; Büchner, B.; Grüneis, A. *Nano Lett.* **2010**, *10*, 3360.

(32) Ryu, S. M.; Han, M. Y.; Maultzsch, J.; Heinz, T. F.; Kim, P.; Steigerwald, M. L.; Brus, L. E. *Nano Lett.* **2008**, *8*, 4597.

(33) Nair, R.; Ren, W.; Jalil, R.; Riaz, I.; Kravets, V.; Britnell, L.; Blake, P.; Schedin, F.; Mayorov, A. S.; Yuan, S.; Katsnelson, M. I.; Cheng, H. M.; Strupinski, W.; Bulusheva, L. G.; Okotrub, A. V.; Grigorieva, I. V.; Grigorenko, A. N.; Novoselov, K .S.; Geim, A. K. *Small* **2010**, *6*, 2877−2884.

(34) (a) Leenaerts, O.; Peelaers, H.; Hernández-Nieves, A. D.; Partoens, B.; Peeters, F. M. *Phys. Rev. B* **2010**, *82*, 195436. (b) Withers, F.; Dubois, M.; Savchenko, A. K. *Phys. Rev. B* **2010**, *82*, 073403. (c) Şahin, H.; Topsakal, M.; Ciraci, S. *Phys. Rev. B* **2011**, *82*, 115432. (d) Tang, S. B.; Zhang, Z. Y. *J. Phys. Chem. C* **2011**, *115*, 16644−16651. (e) Ueta, A.; Tanimura, Y.; Prezhdo, O. V. *J. Phys. Chem. C* **2012**, *116*, 8343−8347.
(35) Samarakoon, D. K.; Chen, Z. F.; Nicolas, C.; Wang, X. Q. *Small* **2011**, *7*, 965−969.
(36) Spanu, L.; Sorella, S.; Galli, G. *Phys. Rev. Lett.* **2009**, *103*, 196401.
(37) Lebègue, S.; Harl, J.; Gould, T.; Ángyán, J. G.; Kress., G.; Dobson, J. F. *Phys. Rev. Lett.* **2010**, *105*, 196401.
(38) Barone, V.; Hod, O.; Peralta, J. E.; Scuseria, G. E. *Acc. Chem. Res.* **2011**, *44*, 269−279.
(39) Marini, A.; García-González, P.; Rubio, A. *Phys. Rev. Lett.* **2006**, *96*, 136404.
(40) Marom, N.; Bernstein, J.; Garel, J.; Tkachenko, A.; Joselevich, E.; Kronik, L.; Hod, O. *Phys. Rev. Lett.* **2010**, *105*, 046801.
(41) Bučko, T.; Hafner, J.; Lebègue, S.; Ángyán, J. G. *J. Phys. Chem. A* **2010**, *114*, 11814−11824.
(42) Tang, Q.; Li, F. Y.; Zhou, Z.; Chen, Z. F. *J. Chem. Phys. C* **2011**, *115*, 11983−11990.
(43) Hod, O. *J. Comp. Theor. Chem.* **2012**, *8*, 1360−1369.
(44) Echeverría, J.; Aullón, G.; Danovich, D.; Shaik, S.; Alvarez, S. *Nat. Chem.* **2011**, *3*, 323−330.
(45) Fokin, A. A.; Gerbig, D.; Schriner, P. R. *J. Am. Chem. Soc.* **2011**, *133*, 20036−20039.
(46) Grimme, S.; Antony, J.; Ehrlich, S.; Krieg, H. *J. Chem. Phys.* **2010**, *132*, 154104.
(47) Frisch, M. J.; et al.. *Gaussian 09*; Gaussian, Inc.: Wallingford, CT, 2009. See the Supporting Information for the full reference.
(48) Baldridge, K. K.; Peverati, R. *J. Chem. Theory Comput.* **2008**, *4*, 2030−2048.
(49) Sameera, W. M. C.; Maseras, F. *Phys. Chem. Chem. Phys.* **2011**, *13*, 10520−10526.
(50) Wheeler, S. E. *J. Am. Chem. Soc.* **2011**, *133*, 10262−10274.
(51) Raju, R. K.; Bloom, J. W. G.; An, Y.; Wheeler, S. E. *ChemPhysChem* **2011**, *12*, 3116−3130.
(52) (a) Head-Gordon, M.; Pople, J. A. *Chem. Phys. Lett.* **1988**, *153*, 503−506. (b) Frisch, M. J.; Head-Gordon, M.; Pople, J. A. *Chem. Phys. Lett.* **1990**, *166*, 275−280. (c) Frisch, M. J.; Head-Gordon, M.; Pople, J. A. *Chem. Phys. Lett.* **1990**, *166*, 281−289.
(53) (a) Delley, B. *J. Chem. Phys.* **1990**, *92*, 508−517. (b) Delley, B. *J. Chem. Phys.* **2000**, *113*, 7756−7764.
(54) Perdew, J. P.; Burke, K.; Ernzerhof, M. *Phys. Rev. Lett.* **1996**, *77*, 3865−3868.
(55) Perdew, J. P.; Wang, Y. *Phys. Rev. B* **1992**, *45*, 13244−13249.
(56) Hehre, W. J.; Radom, L.; Schlyer, P. v. R.; Pople, J. A. *Ab initio Molecular Orbital Theory*; Wiley: New York, 1986.
(57) Grimme, S. *J. Comput. Chem.* **2007**, *27*, 1787−1799.
(58) Zacharia, R.; Ulbricht, H.; Hertel, T. *Phys. Rev. B* **2004**, *69*, 155406.
(59) Li, X. S.; Liu, L.; Schlegel, H. B. *J. Am. Chem. Soc.* **2002**, *124*, 9639−9647.
(60) Zhu, L. Y.; Yi, Y. P.; Li, Y.; Kin, E. G.; Coropceanu, V.; Brédas, J. L. *J. Am. Chem. Soc.* **2012**, *134*, 2340−2347.
(61) Thonhauser, T.; Cooper, V. R.; Li, S.; Puzder, A.; Hyldgaard, P.; Langreth, D. C. *Phys. Rev. B* **2007**, *76*, 125112.
(62) (a) Son, Y.-W.; Cohen, M. L.; Louie, S. G. *Nature* **2006**, *444*, 347−349. (b) Kan, E. J.; Li, Z. Y.; Yang, J. L.; Hou, J. G. *Appl. Phys. Lett.* **2007**, *91*, 243116. (c) Hod, O.; Barone, V.; Peralta, J. E.; Scuseria, G. E. *Nano Lett.* **2007**, *7*, 2295−2299. (d) Hod, O.; Scuseria, G. E. *ACS Nano* **2008**, *2*, 2243−2249. (e) Park, C. H.; Louie, S. G. *Nano Lett.* **2008**, *8*, 2200−2203. (f) Huang, B.; Son, Y. −W.; Kim, G.; Duan, W. H.; Ihm, J. *J. Am. Chem. Soc.* **2009**, *131*, 17919−17925. (g) Kou, L. Z.; Li, C.; Zhang, Z. H.; Guo, W. L. *ACS Nano* **2010**, *4*, 2124−2128. (h) Lee, Y.-L.; Kim, S.; Park, C.; Ihm, J.; Son, Y.-W. *ACS Nano* **2010**, *4*, 1345−1350.
(63) Zhou, J.; Wang, Q.; Sun, Q.; Jena, P.; Chen, X. S. *Proc. Natl. Acad. Sci. U.S.A.* **2010**, *107*, 2801−2806.